

The Effects of Elevated CO₂ Concentrations on Cell Division Rates, Growth Patterns, and Blade Anatomy in Young Wheat Plants Are Modulated by Factors Related to Leaf Position, Vernalization, and Genotype

Josette Masle*

Research School of Biological Sciences, Institute of Advanced Studies, Australian National University, Canberra, Australian Capital Territory 2601, Australia

This study demonstrates that elevated [CO₂] has profound effects on cell division and expansion in developing wheat (*Triticum aestivum* L.) leaves and on the quantitative integration of these processes in whole-leaf growth kinetics, anatomy, and carbon content. The expression of these effects, however, is modified by intrinsic factors related to genetic makeup and leaf position, and also by exposure to low vernalizing temperatures at germination. Beyond these interactions, leaf developmental responses to elevated [CO₂] in wheat share several remarkable features that were conserved across all leaves examined. Most significantly: (a) the contribution of [CO₂] effects on meristem size and activity in driving differences in whole-blade growth kinetics and final dimensions; (b) an anisotropy in cellular growth responses to elevated [CO₂], with final cell length and expansion in the paradermal plane being highly conserved, even when the rates and duration of cell elongation were modified, while cell cross-sectional areas were increased; (c) tissue-specific effects of elevated [CO₂], with significant modifications of mesophyll anatomy, including an increased extension of intercellular air spaces and the formation of, on average, one extra cell layer, while epidermal anatomy was mostly unaltered. Our results indicate complex developmental regulations of sugar effects in expanding leaves that are subjected to genetic variation and influenced by environmental cues important in the promotion of floral initiation. They also provide insights into apparently contradictory and inconsistent conclusions of published CO₂ enrichment studies in wheat.

The consequences for plant growth and morphogenesis of variations in photosynthesis depend on the efficiency of the conversion of triose-P into Suc and of phloem loading at the sites of Suc production and unloading in growing sinks. Ultimately, however, they depend on the sensitivity to sugar supply of a suite of developmental processes involved in meristem initiation, cell division, expansion, and differentiation, and of the mechanisms that regulate the integration of these processes in the formation of organs with a certain shape, size, and structure. The aim of the present study was to investigate this latter area using atmospheric [CO₂] as a tool for manipulating sugar supply to expanding organs and wheat (*Triticum aestivum* L.) as a model experimental system.

Based on experiments at the whole-plant or whole-leaf level, it has been reported that, relative to other species, wheat is not very responsive to elevated [CO₂], especially at early stages. It has been argued (Nicolas et al., 1993; Christ and Körner, 1995; Slafer and Rawson, 1997) that while it enhances tillering by promoting the development of axillary meristems, elevated [CO₂] has little to no effect on leaf development and growth in wheat, a conclusion also recently put forward for rice, another important cereal (Jitla et al., 1997). These reports challenged the evidence from other studies using wheat and a range of other species showing greatly increased aerial growth rates caused by elevated [CO₂] in very young seedlings, which progressively decrease concurrently with changes in carbon partitioning (e.g. wheat [Neales and Nicholls, 1978; Masle et al., 1990]; soybean [Rogers et al., 1984]; cotton [Wong et al., 1992]; tobacco [Masle et al., 1993]). They were also intriguing in the face of the profound developmental effects of exposure to elevated [CO₂] or of Suc feeding recently documented at the cellular and subcellular levels in leaves of several species, including wheat (e.g. Robertson and Leech, 1995; first leaf of 7-d-old seedlings) and sugar beet (Kovtun and Daie, 1995; leaves of 4-week-old seedlings).

The aim of the work presented here was to examine the effects of elevated [CO₂] on the spatial and temporal patterns of cell division and cell expansion in developing wheat leaves and on their translation into variations of whole-leaf growth kinetics, anatomical features, and carbon content. The analysis was conducted in two genotypes. Vernalization was used as a way of shifting the timing of floral initiation and associated changes in carbon allocation within the plant (e.g. Griffiths and Lyndon, 1985).

MATERIALS AND METHODS

Growth Conditions

Wheat (*Triticum aestivum* L.) plants were grown from seed in two adjacent, well-ventilated greenhouses matched for temperature (23°C ± 0.1°C SE day and night) and relative humidity (62% ± 1.0% during the day and 52% ± 1.2% at night), but providing contrasted atmospheric CO₂ concentrations. One greenhouse was run at present ambient CO₂ concentrations, i.e. on a typical day, 350 ± 10 ppm

* E-mail masle@rsbs.anu.edu.au; fax 61-2-6249-4919.

during the day and 420 ± 19 ppm at night, while the other greenhouse was run at an elevated CO_2 concentration of 900 ± 12 ppm, day and night. Day length increased slowly over the duration of the experiment (4 weeks) from 11 to 12 h according to seasonal variations in Canberra, Australia at that time of the year (August to September). The incident radiation varied from day to day according to outside conditions around a daily average of $718 \pm 40 \mu\text{mol quanta m}^{-2} \text{s}^{-1}$, but was stable over the whole formation of the leaves used for growth kinematic analysis (see below).

Two wheat cultivars of contrasting genetic background, morphology, and growth habit were used: cv Hartog, a selection from the CIMMYT (Centro Internacional de Mejoramiento de Maiz y Trigo) variety Pavon 76, carrier of the Rht2 dwarf gene and classified as a spring wheat, and cv Birch 75, a true winter wheat derived from crosses between English and CIMMYT lines. cv Birch and cv Hartog seeds were germinated in Petri dishes on wet filter paper and vernalized at 2°C to 3°C in the dark in a cold room for 7 weeks. By then, seminal roots were 30 to 40 mm long, and the first leaf 20 to 40 mm long. Five days before sowing, another batch of seeds was germinated in similar conditions and kept in the dark at 23°C to obtain non-vernalized "control" seedlings of similar size at sowing as the vernalized ones. All seedlings were transplanted on the same day to pots filled with a 1:2 sand:perlite mix saturated with nutrient solution (Hewitt and Smith, 1975). Pots were flushed once or twice daily with full-strength nutrient solution kept at greenhouse temperature.

Destructive Growth Measurements

Plants of cv Birch and cv Hartog were harvested from each greenhouse on d 1, 3, 8, d 15 to 17 (date of sampling for detailed kinematic analysis of leaf elongation, see below), and finally on d 23 (cv Birch) or d 27 (cv Hartog). On d 3 and 8, only non-vernalized plants were sampled; on the other dates, both vernalized and non-vernalized plants were harvested. Roots were cut at the crown level; individual tillers were identified according to their position on the plant (Masle, 1984) and separated. Leaf blade areas were immediately measured using an area meter (LI-3000, LI-COR, Lincoln, NE) and dry weights were determined after 48 h of oven drying at 80°C . These measurements were done on each tiller individually, except at the final harvest, when tillers were bulked according to their biological age (Masle, 1984). The experiment was terminated when leaf 6 was fully mature (i.e. leaf 8 had just appeared).

Kinematic Analysis of Leaf Elongation

Leaf elongation rates were analyzed non-destructively through daily measurements of the lengths of all visible leaves to the nearest 0.5 mm. The underlying cellular responses were investigated using the kinematic approach pioneered by Goodwin and Stepka (1945) and Erickson and Sax (1956) for the analysis of axial growth. This method is based on the principles of fluid dynamics, and treats the production of cells and their displacement analogously to those of physical elements within a fluid. It is particularly

well suited to cereals and, more generally, grass leaves, where most of the leaf tissue is generated by a well-defined basal growth zone made of parallel cellular files whose expansion is mostly unidirectional and in which division and elongation occur in two distinct segments. In constant environments, the blade elongation rate after emergence from older sheaths is constant (e.g. Friend et al., 1962); moreover, the spatial distribution of epidermal cell lengths in the growth zone and the size of that zone (no. of constitutive cells) remain unchanged (data not shown; Schnyder et al., 1990; Beemster et al., 1996). In these "steady-state conditions," the spacing of transverse cell walls along the growth zone can be used to determine cell elongation rates with respect to both physical position and biological age, including meristematic cells (Beemster et al., 1996). From the spatial distribution of newly formed walls in the division zone, local cell partitioning rates can also be derived.

Leaf Elongation Rate, Cell Length Profile, and Size of the Growth Zone

Leaf 6 was selected for this analysis. Following blade emergence, leaf length was measured every 3 h over a full day/night cycle. A regression line was fitted through these measurements over time ($r^2 > 0.999$ in all cases), and the slope of that line was taken as a measurement of the leaf linear rate of elongation (E). Twenty-four hours after blade emergence, the leaf was quickly dissected from the plant under the microscope as close as possible to its insertion on the apex. The leaf was then immediately immersed in boiling methanol until all chlorophyll had been removed and then cleared in lactic acid. Five leaves were analyzed for each treatment (2 vernalization levels \times 2 CO_2 concentrations \times 2 genotypes). Because of $[\text{CO}_2]$ and vernalization effects on the rate of leaf development (see "Results"), leaves 6 were not all synchronized and were, depending on treatment, sampled over 2 d (d 15–17).

The cleared leaf was mounted on a light microscope (axioscope, Zeiss, Jena, Germany) fitted with a video camera (model WV-CL 702E, Panasonic, Tokyo). A file of epidermal cells of the same type for all leaves (file of sister cells adjacent to a stomatal row) was selected and individual cell lengths were measured throughout the growth zone. This was done from video images using the morphometric program MTV (Datacrunch, San Clemente, CA). Note was taken of the position of thin transverse cell walls, which are indicative of recent cell divisions. Such walls were typically visible only in the basal 4 to 7 mm of the growth zone. The position of the most distal fresh wall was taken as defining the transition between the division and the elongation-only zone, where cells had lost the ability to divide and were starting to undergo rapid expansion. In many leaves, the last divisions were "asymmetrical," yielding two daughter cells of very unequal length. The shortest daughter cells could easily be traced through the elongation zone, where they hardly expanded and started to differentiate into trichomes. The positions from the base of the leaf (x_0) of the last symmetrical and asymmetrical divisions were denoted as x_{sd} and x_{ad} , respectively. Individual cell lengths were also measured along a 10-mm seg-

ment of mature blade and their average was taken as an estimate of final cell length, l_f . Individual cell lengths, $l(x)$, and individual elemental lengths, $l(x)^*$ (the length of a cell and its associated trichome), were plotted against position (x) along the growth zone. In the elongation-only zone, cell lengths were fitted by a Richards function as in Morris and Silk (1992) for cells and Beemster et al. (1996) for elements. The distal end of the growth zone was defined as the location (x_{el}) where the fitted cell length reached 95% of l_f . For the meristem, where cell length does not bear any direct relationship to position, cell length data were smoothed by calculating moving averages over 11 cell intervals around x . The number of meristematic cells along a file in the leaf growth zone were denoted as N_{sd} and N_{ad} for the zones of symmetrical and asymmetrical divisions, respectively, and the number of elongating-only cells was denoted as N_{el} .

Growth Velocities and Strain Rates

The velocities of displacement $v(x)$ and relative cell elongation rates $r(x)$, the latter often referred to as strain rates in the kinematic literature, can be calculated as a function of position x . Velocities in the elongation-only zone are given by equation 11 in Morris and Silk (1992):

$$v(x) = F.l(x) \quad (1)$$

where F is the cell flux, i.e. the number of cells passing through x per unit of time, and $l(x)$ are the fitted cell lengths obtained as described above. During steady growth, F is constant throughout the elongation zone; the number of cells displaced out of the meristem into the elongation zone is equal to the number of cells moving out of the growth zone and is given by:

$$F = \frac{v(x_{el})}{l_f^*} = \frac{E}{l_f^*} \quad (2)$$

where l_f^* denotes final elemental length (length of mature cell and its associated trichome).

In the meristem, Equation 1 becomes:

$$v(x) = \phi(x).F.l(x) \quad (3)$$

where $\phi(x)$ is the number of newly formed cross-walls between the base of the meristem and position x as a proportion of such walls from the base to x_{sd} (Beemster et al., 1996).

The relative elongation rates $r(x)$ are the derivatives of velocities with respect to position (equation 2 in Morris and Silk, 1992):

$$r(x) = \frac{dv}{dx} \quad (4)$$

In the elongation zone, time versus position relationships can easily be calculated. The time, $t(x)$, taken for a cell to be displaced from x_{sd} (the meristem) to a further particular position, x , in the elongation zone is given by:

$$t(x) = c.n(x) \quad (5)$$

where $n(x)$ is the total number of cells between x_{sd} and x and c is the cellochron, the time taken for a cell to be displaced by one position (Silk et al., 1989).

$$c = \frac{1}{F} \quad (6)$$

and

$$n(x) = \int_{x_{sd}}^x \frac{dx}{l(x)} \quad (7)$$

The residence time of a cell in the elongation-only zone, T_{el} , was calculated as:

$$T_{el} = c.N_{el} \quad (8)$$

Cell Partitioning Rates

The average cell partitioning rate, \bar{p} , in the zone of symmetrical division and its inverse, the average cell cycling time, \bar{t}_c , time elapsed between two successive divisions, were calculated as in Green (1976):

$$\bar{p} = \frac{F}{N_{sd}} \quad \text{and} \quad \bar{t}_c = \frac{N_{sd}}{F} \quad (9)$$

or

$$\bar{t}_c = N_{sd}.c$$

Local symmetrical partitioning rates at any location x along the meristem, $p(x)$, were calculated according to the method of Beemster et al. (1996) as the average partitioning rate over intervals (i) of m cells around the cell at location x , using:

$$p(i, x) = \frac{\phi(i, x)}{m} F \quad (10)$$

where $\phi(i, x)$ denotes the number of newly formed cross walls found in interval i , as a proportion of the total number of such walls from x_o to x_{sd} . Calculations were done on intervals of 20 cells.

Quantitative Analysis of Mature Blade Anatomy

At final harvest, mature blades of leaf 6 were sampled for detailed anatomical observations. Four contiguous short segments, each about 3 mm long (denoted segment 1–4 below), were taken mid-length along the blade.

Morphometric Analysis of Cleared Mature Epidermis

Segment 1 was cleared in methanol and lactic acid as described above. The numbers of epidermal files between veins 1 and 2, 2 and 3, and 3 and 4 were counted (veins numbered from the mid-rib). An 800- μm -long field of view delimited by veins 2 and 3, equivalent to 0.2 to 0.3 mm² of leaf tissue, was selected on the abaxial side of the blade for determining the densities and relative proportions of the

various types of cells constituting the mature epidermis (stomata and interstomatal cells, sister cells in adjacent rows, elongated non-specialized cells, and trichomes). The length and maximum width of 10 contiguous cells of each type were measured, excluding stomata and trichomes. This was replicated three times per leaf.

Morphometric Analysis of the Mesophyll Tissue on Leaf Sections

Segments 2 and 3 were immediately fixed in 2% (v/v) glutaraldehyde in 50 mM 1,4-piperazinediethanesulfonic acid (PIPES) buffer for 3 h (1 h of which was under vacuum), post-fixed in 1% (v/v) osmium tetroxide in 25 mM phosphate buffer, pH 7.0, slowly dehydrated in ethanol, and embedded in Spurr's resin. Three-micrometer-thick cross-sections (segment 2) and longitudinal sections (segment 3) were cut, stained with toluidine blue, and mounted on a microscope fitted with a video camera for morphometric measurements. Cross-sections were used to determine the number of mesophyll cell layers and accurately measure the thicknesses of the whole blade, mesophyll tissue, and each epidermis, and the cross-sectional areas of individual mesophyll and epidermal cells. These parameters were measured at three positions across the blade centered mid-way between veins 1 and 2, 2 and 3, and 3 and 4. At each position the individual cross-sectional areas (a_i) of all mesophyll cells comprised within a small rectangle of total area A were measured. The difference $1 - \sum_{i=1}^p a_i / A$ was calculated as an estimate of the proportion of tissue cross-sectional area occupied by air spaces. Depending on treatment, the number of mesophyll cells, p , measured at each location varied from 12 to 20. Four sections were analyzed at each of three locations across the embedded segment, and there were four replicated leaves per treatment. Mesophyll cell lengths were measured on 3- μ m longitudinal sections cut parallel to veins. In wheat, mesophyll cells are elongated with several deep lobes (e.g. Parker and Ford, 1982), so mesophyll cell lengths were only measured for cells whose end walls were clearly visible and abutting the adjacent cells in the file.

Estimation of Mesophyll Cell Numbers

Segment 4 (segment symmetrical to segment 3 with respect to mid-rib) was used to estimate mesophyll cell num-

bers. The slice of fresh tissue was fixed in 3.5% (v/v) glutaraldehyde for 1 h at room temperature, then transferred into 0.1 M EDTA (pH 9.0), incubated for 3 h at 60°C, and stored at 4°C. The slice of tissue was later macerated in 5% (w/w) chromium trioxide at 4°C for 24 h until cells could be easily teased apart without damage. Mesophyll cell counts were made a few days later using a 0.1-mm-depth hemocytometer under a microscope (Zeiss) on five loadings per leaf and four leaves per treatment.

Sugar Analyses

Soluble sugars and starch were extracted twice from dried blade and root powder in 80% (v/v) ethanol. Color pigments were removed by the addition of activated charcoal (Norit SA3, Aldrich Company, Milwaukee, WI) to the extract, followed by centrifugation at 12,000 rpm for 10 min. The supernatant was dried down and resuspended in water. Glc, Fru, and Suc concentrations were determined enzymatically in three steps after the addition of a formulation of hexokinase and Glc-6-P dehydrogenase (Glc [HK] diagnostics reagent, Sigma-Aldrich, St. Louis) and of invertase and isomerase. Glc moieties were measured spectrophotometrically at 340 nm following each reaction.

Statistics

Treatment effects on kinematic and morphometric parameters were assessed by analysis of variance using General Linear Models algorithms (statistical package GLIM, version 3.77, 1985, Royal Statistical Society, London). In addition, differences in the spatial distributions of strain rates and partitioning rates were compared by the test of Kolmogorov-Smirnov.

RESULTS

[CO₂] Effects on Whole-Plant Growth, Carbon Accumulation, and Leaf Expansion

Plants under 900 ppm [CO₂] grew significantly more than those under 350 ppm (Table I), showing a 52% to 93% increase in total dry weight at the end of the experiment and a 39% to 82% increase in leaf area. All tillers contributed to that response (Fig. 1), including the main tiller, where a growth stimulation by elevated [CO₂] was detect-

Table I. Influence of growth [CO₂] and vernalization on whole-plant dry weight and leaf area (means and *se* values) at the end of the experiment in cv Birch (d23) and cv Hartog (d27)

Genotype	Vernalization	[CO ₂] ppm	Dry Weight		Leaf Area	
			<i>g</i>	% increase	cm ²	% increase
Birch	Yes	350	0.639 (0.054)		190.2 (18.3)	
		900	1.151 (0.061)	80.1	298.7 (19.3)	57.1
	No	350	0.800 (0.051)		220.0 (15.2)	
		900	1.218 (0.051)	52.3	305.4 (9.4)	38.9
Hartog	Yes	350	0.717 (0.040)		210.6 (11.0)	
		900	1.385 (0.087)	93.2	383.7 (21.6)	82.2
	No	350	1.063 (0.055)		294.3 (13.9)	
		900	2.031 (0.101)	91.1	529.8 (22.0)	80.0

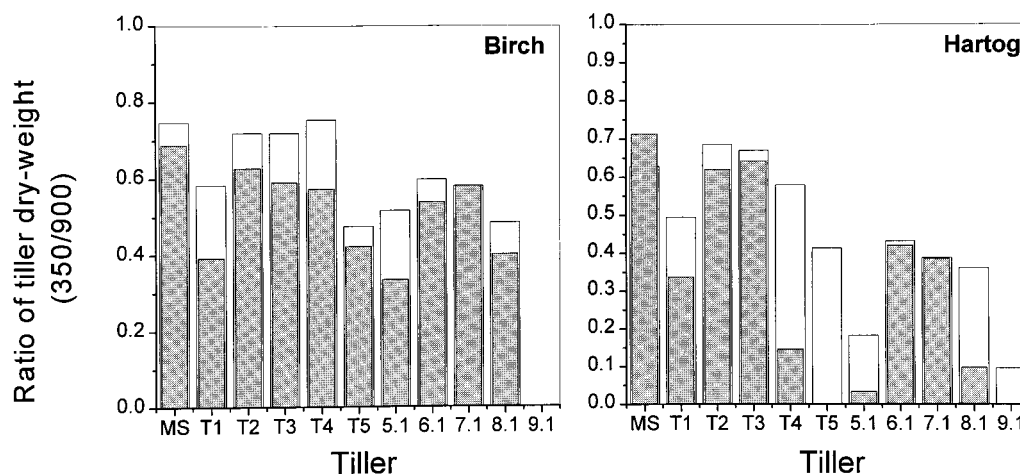


Figure 1. Ratio of tiller dry weights under 350 ppm CO₂ to tiller dry weights under 900 ppm CO₂ at final harvest (d 23 and 27 in cv Birch and cv Hartog, respectively). Labels on the x axis refer to the main tiller (MS) followed by the five first primary tillers (T1–T5) and tillers of higher order grouped according to biological age (labels 5.1–8.1, corresponding to tillers that normally emerge concurrently with tiller T3–T7, respectively, and with leaves 6 to 9 on the main tiller, Masle [1984]). White bars, Ratios for non-vernalized plants; gray bars, ratios for vernalized plants.

able within 4 to 15 d after sowing (Fig. 2) and led to a 25% to 40% increase in dry weight at final harvest (d 23–27). Elevated [CO₂] accelerated the emergence rate of secondary and tertiary tillers (data not shown), leading to plants with a greater number of concurrently expanding sinks at a given time. For those tillers, the size differences shown in Figure 1 therefore reflect the compounded effects of earlier appearance and faster growth rate thereafter. Although elevated [CO₂] led to significant increases in the soluble sugar content in leaves (Fig. 3), this effect was insufficient to fully account for the increased dry weights shown in Table I and Figures 1 and 2.

Figure 4 describes the kinetics of elongation of successive leaves of the main stem, from emergence of the blade to completion of elongation. In the two genotypes examined, and whether seeds had been vernalized or not, increased atmospheric [CO₂] stimulated the expansion growth of individual leaves. Remarkably, however, this stimulatory effect only became visible and significant beyond leaf 2 (vernalized plants) or even leaf 4 (non-vernalized plants). Moreover, although in later leaves elevated [CO₂] systematically resulted in longer mature blades, the underlying reasons varied depending on genotype and vernalization treatment. In vernalized cv Hartog plants, for example, elevated [CO₂] caused earlier blade emergence (see in Fig. 4 the 1–1.5 d lag between the two CO₂ levels for leaves 4–8) and extended growth duration. In the non-vernalized seedlings of the two genotypes, however, these two parameters were not significantly affected by exposure to elevated [CO₂], but the elongation rate of emerged blades was enhanced. In vernalized cv Birch plants, blades emerged earlier and elongated faster thereafter.

Kinematic Analysis of Leaf Elongation

Cell Flux and Mature Cell Length

An analysis of the cellular responses underlying the effects of elevated [CO₂] on leaf elongation was undertaken

in leaf 6. Table II gives the average blade elongation rate (E) over the 24-h period following tip blade emergence. For each individual leaf, E was estimated by the regression line fitted to the three hourly measurements of blade lengths taken during that period (see “Materials and Methods”). Consistent with data shown in Figure 4, E was always greater under 900 ppm than 350 ppm. Vernalization had no significant effect except in cv Birch under high [CO₂]. Variations in E can be analyzed using Equation 2 in relation to variations in F , the flux of cells moving out of the growth zone per unit of time, and in l_f^* , the length of the newly fully expanded elements. Table II shows that elevated [CO₂] caused a 15% to 20% increase in cell flux ($P < 5\%$) irrespective of genotype and vernalization treatment. In cv Birch, F was also affected by vernalization, although to a lesser extent, being 12% greater in non-vernalized than in vernalized seedlings. In contrast, final elemental lengths and final cell lengths were remarkably stable across growth [CO₂] levels, vernalization treatments, and genotype (see Table II; actual overall mean cell length $200 \pm 10 \mu\text{m}$; predicted mean from the analysis of variance = $199.6 \pm 2.8 \mu\text{m}$).

Elevated [CO₂] increased the total elongation rate occurring in both the division zone and the elongation-only zone distal to it (E_{sd} and E_{el} , respectively) except in cv Hartog under vernalization, where E_{sd} was similar in high- and low-[CO₂]-grown leaves (data not shown). The relative contributions of meristematic and elongating-only cells to the overall leaf elongation rate, E , were only slightly affected by growth [CO₂] or vernalization, varying between 10% to 15% and 90% to 85%, respectively.

Meristem Size and Cell Partitioning Rates

By definition during steady growth the flux of cells moving out of the growth zone is equal to the number of cells displaced out of the meristem into the elongation-only zone during the same period. It therefore integrates variations in both the number of meristematic cells and their

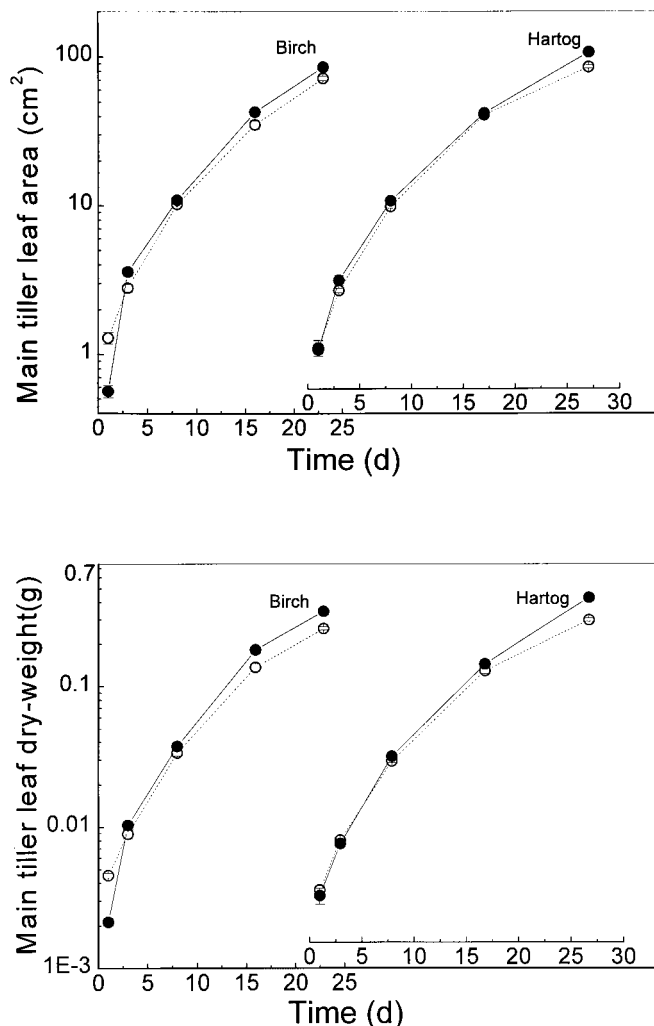


Figure 2. Main tiller leaf area (top panel) and dry weight (bottom panel) plotted as a function of time (days from sowing) for the non-vernallized seedlings of cv Birch and cv Hartog grown under 350 (○) and 900 ppm [CO₂] (●); bars across symbols represent 2 SE. Note that the y axis is common to the two genotypes and is in log-scale.

partitioning rate (Eq. 9). In cv Birch, the average interval between two successive divisions, \bar{t}_c (calculated using Eq. 9), was 3 to 4 h shorter under 900 compared with 350 ppm CO₂, equivalent to an approximately 13% reduction (Table III), and the number of symmetrically dividing cells per file (N_{sd}) was increased, although relatively less so (+8%; $P < 0.05$) (Table III). In cv Hartog, elevated [CO₂] had, qualitatively, similar effects; their relative importance, however, depended on vernalization treatment (Table III). In vernalized cv Hartog seedlings, faster cycling rates were the dominant response (14% decrease in \bar{t}_c versus an 8% increase in N_{sd}), as was also seen in cv Birch, while in the absence of vernalization, elevated [CO₂] had only a weak effect on \bar{t}_c (5%, non-significant decrease), but caused a 20% increase in meristematic cell number. Even when individually non-statistically significant, the combined effects of elevated [CO₂] on \bar{t}_c and N_{sd} always gave rise to highly significant differences in cell fluxes between low- and high-[CO₂]-grown plants (Table II).

The local partitioning rates calculated using the distribution of fresh cell walls (Eq. 10) suggest the existence of a spatially non-uniform field of responses to elevated [CO₂] along the meristem. As illustrated in Figure 5a, elevated [CO₂] typically enhanced partitioning rates mostly in the basal 2 to 3 mm of the meristem while having little effect in the most proximal segment.

Size of the Leaf Growth Zone: Kinetics of Cell Elongation

Elongation in the Meristem. Elevated [CO₂] had no significant effect on the distributions of meristematic cell lengths in either genotype or vernalization treatment (Fig. 6, insets). Variation in meristem length was therefore highly correlated to variations in meristematic cell number. Consistent with the variations of N_{sd} described earlier, elevated [CO₂] systematically increased the longitudinal extension of the division zone ($P < 5\%$), especially in the non-vernallized seedlings of cv Hartog (Table III, L_{sd} values). Elevated [CO₂] also enhanced local elongation rates in the meristem; however, as for partitioning rates, this effect was mostly confined to the basal 2 to 3 mm of the meristem (Fig. 5b).

Cell length at division can be estimated from the lengths of freshly formed daughter cells separated by thin transverse cell walls, and was similar in low- and high-[CO₂]-grown leaves ($20.4 \pm 1.8 \mu\text{m}$). Therefore, elevated [CO₂] caused similar proportional increases in the partitioning rate and elongation rate of meristematic cells. Figure 5 (example is of cv Birch) illustrates that the distributions of those two parameters mirrored each other, with the enhancing effect of elevated [CO₂] being confined to the basal half of the meristem.

Elongation of Non-Meristematic Cells. In non-vernallized seedlings, the length of the elongation-only zone (L_{el}) and cell lengths profiles within it and therefore the number of constitutive cells (N_{el}) were not significantly affected by variations in growth [CO₂] (Table III; Fig. 6). The temporal pattern of cell elongation was, however, modified; maximum cell elongation rates were increased (Fig. 7, $P < 5\%$) and the duration of cell elongation was significantly shortened (see T_{el} values in Table III). In contrast, in vernalized seedlings, high [CO₂] increased the length of the elongation zone and the size of the cohort of concurrently elongating cells (N_{el} , Table III), but did not significantly affect maximum cell elongation rates (Fig. 7) nor cell residence times in the elongation zone (Table III). In cv Birch, however, elevated [CO₂] caused maximum cell elongation rates to occur relatively further in the elongation zone (Fig. 7) and later in the expansion time span of the cell (+6 h corresponding to a 20% delay compared with cells of low-[CO₂]-grown leaves) so that within the basal two-thirds of the elongation zone, cells were shorter than under 350 ppm CO₂ (Fig. 6).

Anatomy of Mature Blades

The above data described growth kinetics of epidermal sister cells. Morphometric analysis of cleared epidermis and blade sections allowed examination of the final dimen-

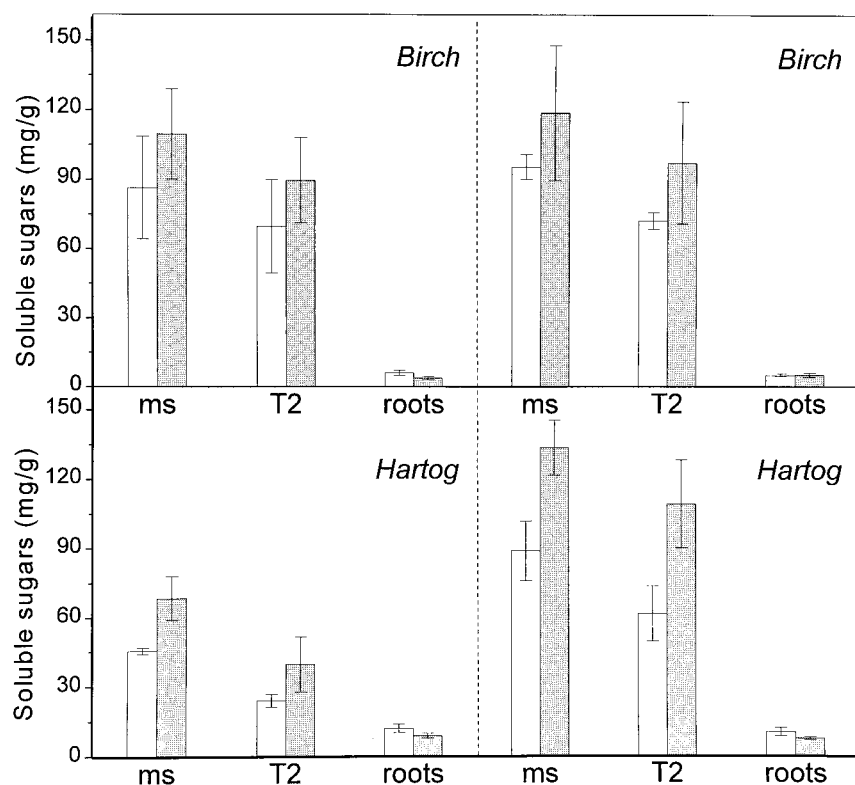


Figure 3. Soluble sugar contents (mg g^{-1} dry weight; means \pm SE) measured on d 23 (cv Birch) or d 27 (cv Hartog) in the main tiller (ms), second primary tiller (T₂), and in roots under 350 (white bars) and 900 ppm [CO₂] (gray bars) in vernalized (left) and non-vernalized (right) seedlings. Glc, Fru, and Suc were measured individually but the two hexoses were present at very low concentrations (≤ 5 mg/g).

sions of other cell types and of blade anatomy. As found for sister cells, the lengths of other epidermal cell types (interstomatal cells and non-specialized elongated cells) did not differ significantly between low- and high-[CO₂]-grown blades (data not shown). The densities of these three cell types were also similar (Fig. 8), implying that their surface area and width were also insensitive to ambient [CO₂]. Stomatal indices or densities were also not affected (Fig. 8). The only significant effect of elevated [CO₂] was a reduction of trichome frequency in the non-vernalized leaves of cv Hartog (trichome index reduced from 9.8%–3.9%). Interestingly, vernalization also had little effect on epidermis anatomy (Fig. 8).

Contrary to our expectations based on observations of cleared epidermis, the examination of blade sections revealed several striking anatomical differences between leaf tissue generated under 350 or 900 ppm CO₂, which also depended on both genotype and vernalization. While consistently having no effect on mesophyll cell length or cell projected area (Table IV), elevated [CO₂] caused a significant increase in the cross-sectional areas of those cells except in the cv Hartog non-vernalized seedlings (Fig. 9, top panel). No such increase was observed in epidermal cells except in the non-vernalized leaves of cv Birch, where the cross-sectional area of epidermal cells of all types was also greater in high-[CO₂]-grown leaves (Fig. 9, bottom panel). Remarkably, elevated [CO₂] consistently caused an increase in air space volume in the mesophyll tissue. This latter effect was more marked in cv Hartog, and significant at any position across the blade (Fig. 10). In cv Birch, it was closest to the mid-vein while disappearing toward the

blade margins. In addition, elevated [CO₂] caused an increase in the number of mesophyll cell layers (on average, one out of three to five layers in total, data not shown) with the exception, again, of the non-vernalized seedlings of cv Hartog. Overall, these various effects resulted in an increase in blade thickness and structural carbon content per unit leaf area in high-[CO₂]-grown leaves (Fig. 10); in the non-vernalized leaves of cv Hartog, however, increased leaf thickness was confined to the mid-rib region. Because ambient [CO₂] had no effect on the size of major or minor veins (vein diameters of 60–80 μm regardless of [CO₂] and vernalization, data not shown), the ratio of mesophyll tissue volume to vein volume was greater in high-[CO₂]-grown leaves.

DISCUSSION

Elevated [CO₂] Caused an Early Stimulation of Plant Growth and Modified the Development of Individual Leaves

Contrary to earlier conclusions in the literature, wheat proved to be an excellent model system to analyze [CO₂] effects on leaf development. In the two genotypes examined, vegetative growth was increased under 900 ppm CO₂. The stimulatory effect of elevated [CO₂] was detectable early, in the first week after sowing, on leaf area expansion and biomass accumulation, at a time that did not coincide with any specific phenological stage nor necessarily with the beginning of tillering (Fig. 4). Depending on genotype and vernalization, a positive growth response to elevated

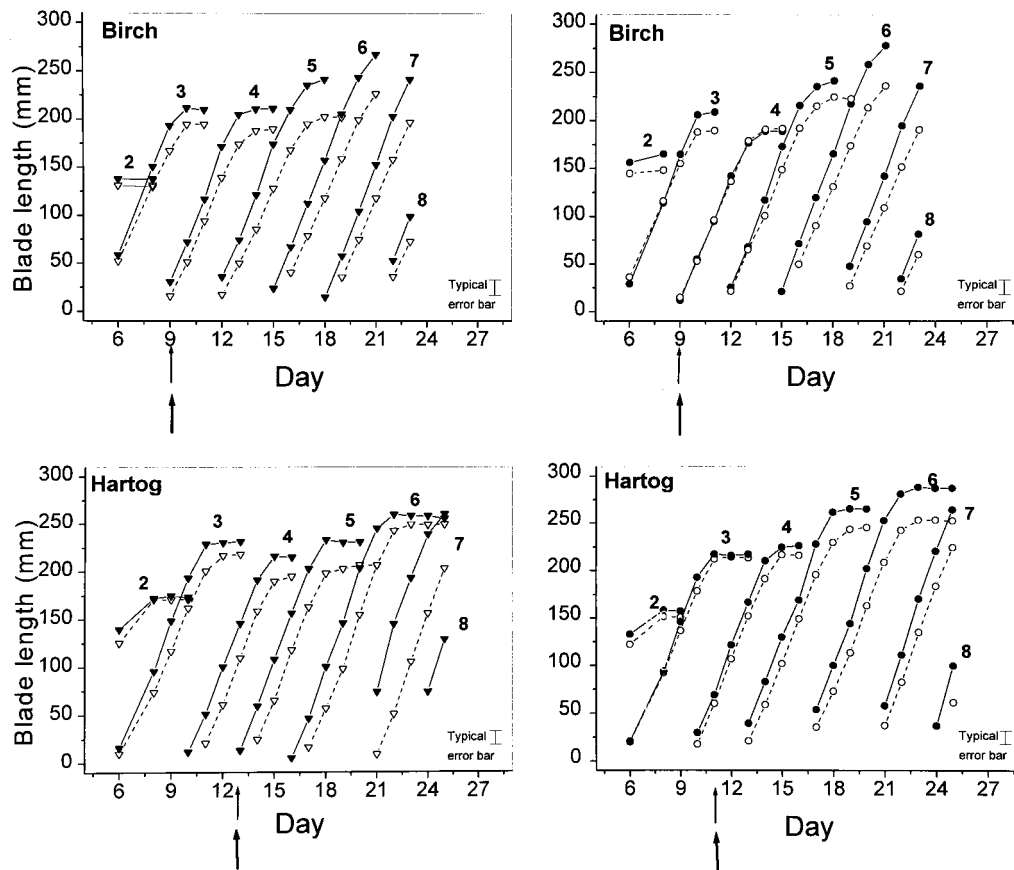


Figure 4. Comparison of blade elongation for successive leaves of the main tiller (leaf 2–8) under 350 (dashed line) and 900 ppm CO₂ (solid line) in vernalized (left) and non-vernalized (right) seedlings of wheat cv Birch and cv Hartog. Blade length was measured from the ligule of the subtending leaf. Arrows on the x axis denote the times of first tiller emergence in low- and high-[CO₂]-grown plants (thin and thick arrows, respectively).

[CO₂] was detected before the appearance of the first tiller (cv Hartog, vernalized leaves), at approximately the same time (e.g. cv Birch, vernalized leaves), or significantly later (e.g. Birch non-vernalized leaves) (Fig. 4). One can therefore conclude that there is no direct causal link between the two events, as has been suggested (e.g. Nicolas et al., 1993; Christ and Körner, 1995). This study demonstrates pro-

found effects of elevated [CO₂] on individual leaves of the main tiller, even before axillary meristems become major competing sinks for carbon. As will be discussed below, these effects are both quantitative and qualitative.

Within a few days after the effects of high [CO₂] on leaf growth were detected, high-[CO₂]-grown plants were characterized by greater ratios of carbon (total or structural)

Table II. Influence of growth [CO₂] and seed vernalization on leaf elongation rate (E), the lengths of mature sister cells or elements (l_i and l_i^* , respectively), and the cell flux (F , number of cells and elements moving in and out of the leaf epidermal elongation zone per unit of time)

[CO₂] and vernalization had statistically significant effects ($P \leq 0.05$) on E and F (values followed by a different letter within a column) but not on l_i and l_i^* (GLM analysis of variance, see "Materials and Methods").

Genotype	Vernalization	[CO ₂]	E	l_i^*	l_i	F
		ppm				
Birch	Yes	350	1.45a	218	210	6.7a
		900	1.70cd	208	201	8.2cd
	No	350	1.54ab	206	201	7.5c
		900	1.89e	205	203	9.2e
Hartog	Yes	350	1.53ab	210	201	7.4b
		900	1.76d	198	189	8.9d
	No	350	1.63bc	206	200	8.0b
		900	1.78d	195	190	9.2d

Table III. Influence of growth [CO₂] and vernalization on the characteristics of the leaf growth zone during the phase of steady elongation following blade tip emergence

The three parameters given for the division zone and the elongation-only zone refer to: the physical extension of these zones (L_{sd} and L_{el}), the number of constitutive cells (N_{sd} and N_{el}), the average cell cycling time, \bar{t}_c , for meristematic cells or residence time in the growth zone (T_{el}) for elongating-only cells. Values followed by a different letter within a column were statistically significantly different ($P \leq 0.05$).

Genotype	Vernalization	[CO ₂]	Division Zone			Elongation-Only Zone		
			N_{sd}	t_c	L_{sd}	N_{el}	T_{el}	L_{el}
		ppm	cells	h	mm	cells	h	mm
Birch	Yes	350	172a	26.1b	3.9a	248a	37.6cd	22.7a
		900	186a	22.9a	4.4b	313b	38.1cd	27.6bc
	No	350	226b	30.5cd	5.0c	266a	35.4c	23.7a
		900	244bc	26.5b	5.7d	257a	27.8a	23.4a
Hartog	Yes	350	268cd	36.9e	6.8e	301b	41.4d	29.6c
		900	290d	32.6d	7.3f	365c	41.2d	33.1d
	No	350	233b	29.5bc	5.7d	296b	37.3cd	26.8b
		900	280d	27.8a	6.6e	290b	32.0b	26.0b

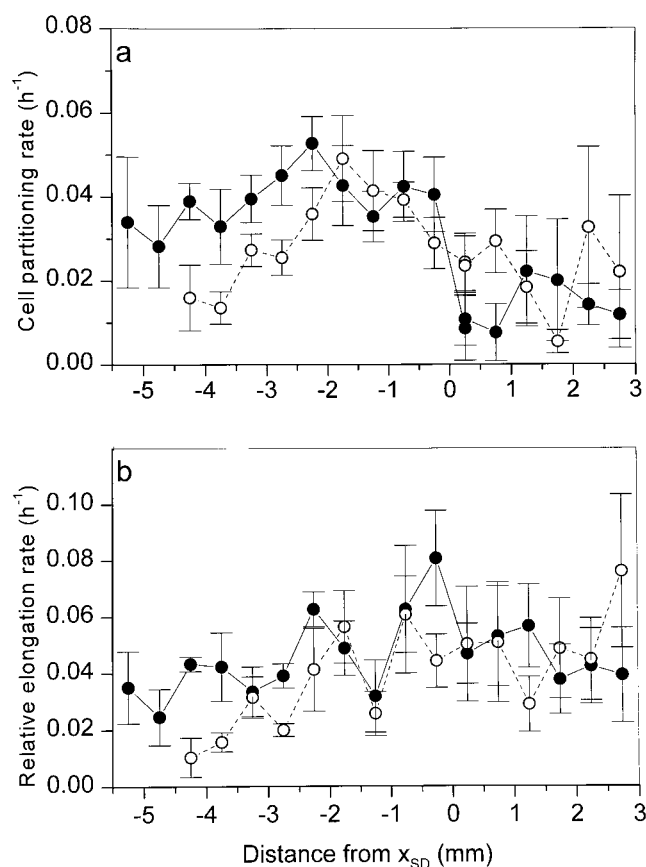


Figure 5. Local cell partitioning rates (a) and relative elongation rates (b) averaged over successive cohorts of 20 cells along the growth zone under 350 and 900 ppm [CO₂] (dashed and solid lines, respectively; vertical bars = 2 SE). Data are for leaf 6 of vernalized cv Birch seedlings; [CO₂] effects followed similar patterns in non-vernalized leaves and also in cv Hartog. On the x axis, positions along the growth zones are described by the distance from the distal end of the division zone, x_{sd} .

laid down in the whole plant to leaf area expanded. These differences mostly reflected an increase in C content per unit leaf area, a feature observed in other CO₂ enrichment studies with wheat or other species and, more generally, in response to increased CO₂ assimilation rates (e.g. Thomas and Harvey, 1983; Vu et al., 1989; Masle et al., 1993). The relative allocation of carbon between roots and shoot was little affected by growth [CO₂]. Higher carbon contents per unit leaf area in high-[CO₂]-grown leaves have been observed in other studies and interpreted as merely reflecting a more advanced stage of development in these leaves, i.e. an ontogenetic drift (see also the "temporal shift model" proposed by Miller et al. [1997]; Sims et al., 1998). In the present study, homologous leaves were characterized by different carbon densities depending on growth [CO₂] not only while expanding, but also when fully mature (Fig. 10).

Our data leave no doubt that there are intrinsic developmental differences between low- and high-[CO₂]-grown leaves, which overall lead to the deposition of more structural carbon per unit leaf area in the latter. Elevated [CO₂] affected cell division and expansion rates (Figs. 5 and 7) and also leaf histogenesis, final dimensions, and anatomy (Figs. 9 and 10). Furthermore, for the first time to our knowledge, it is shown that these quantitative and qualitative effects of elevated [CO₂] on leaf growth are subject to significant intraspecific genetic variation and, most unexpectedly, are modified by seed vernalization, a major developmental cue for the switch between vegetative and reproductive development in cereals.

The effects of atmospheric [CO₂] that are reported here were primarily due to increased photoassimilate supply (see in Fig. 3 the increased sugar contents and the 25% increase in rate of leaf photosynthesis per unit leaf area measured in a preliminary experiment and similar growth conditions). Elevated [CO₂] caused a reduction in stomatal aperture, but, due to the well-ventilated conditions of the greenhouses, there was no detectable difference in leaf temperature between low- and high-[CO₂]-grown plants. Although one cannot totally exclude some role for improved leaf water status under elevated [CO₂], this effect

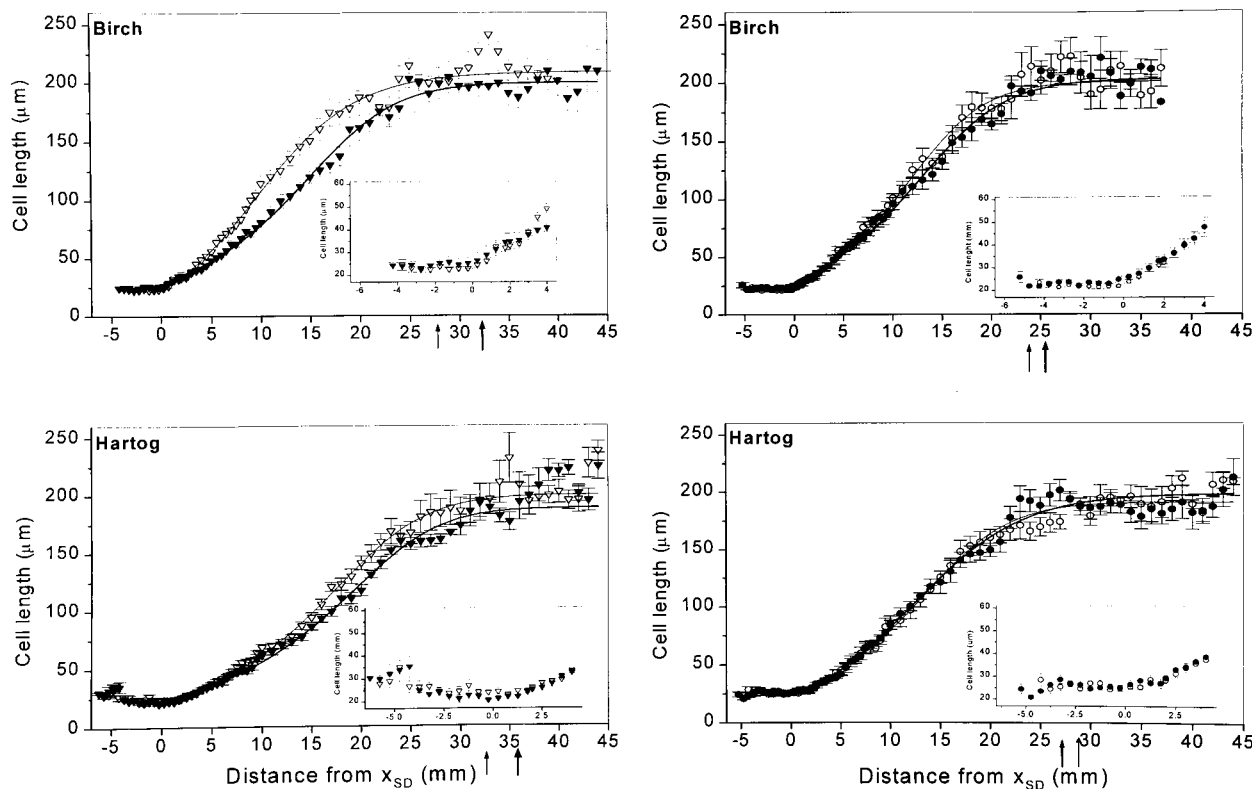


Figure 6. Cell lengths (means and corresponding SE) as a function of position along the growth zone in leaf 6 of vernalized (left) and non-vernalized (right) seedlings of cv Birch and cv Hartog grown under 350 (○) or 900 ppm CO₂ (●). Cell lengths at the base of the growth zones (in the meristem and proximal end of the elongation-only zone) are shown in more detail in the insets. The curves were obtained by fitting the data using a Richards function, as described in "Materials and Methods." Arrows on the x axis denote the position x_{el} , where cell lengths were within 5% of mature cell length under 350 and 900 ppm CO₂ (thin and thick arrows, respectively).

was most likely minor. The soil was maintained very wet and, more importantly, quantitatively similar positive responses to elevated [CO₂] as those described in Figures 1 and 4 were observed in a parallel experiment where plants were grown in hydroponics and under higher air humidity (6–7 mbar leaf-to-air vapor pressure difference against 11–14 mbar in this experiment [J. Masle, unpublished data]).

Cellular Bases of [CO₂] Effects on Leaf Growth and Carbon Deposition per Unit Leaf Area

The cellular responses underlying whole-leaf responses to elevated [CO₂] were examined using a combination of microscopy techniques and the theoretical framework developed earlier for the kinematic analysis of "steady-state" growth zones, characterized by constant cell length profiles (see "Materials and Methods"). All leaves analyzed in the present study were sampled at similar developmental stages during the period of linear elongation that followed blade emergence. The ligule meristem was then just initiated and at 0.5 mm at the most from the base of the leaf, so that the whole growth zone could be treated as one continuous zone for the derivation of kinematic parameters

(Kemp, 1980; Schnyder et al., 1990; Skinner and Nelson, 1995).

Elevated [CO₂] Enhanced (Epidermal) Cell Division Rates

A consistent effect of elevated [CO₂] was to reduce the time interval between successive divisions (Table III). This is the first time that such an effect has been demonstrated in expanding leaves. Earlier studies gave evidence for a direct role of Suc in mitosis in both buds (Ballard and Wildman, 1964) and root meristems (Webster and Henry, 1987), but being based on comparisons of mitotic indices, these data did not allow the separation of the respective contributions of changes in the cell cycle per se versus changes in the number of cycling cells. The present finding of faster cycling rates in leaves expanding under elevated [CO₂] is consistent with the recent report by Kinsman et al. (1997) of enhanced cell division rates in the shoot apex of *Dactylis* under 700 ppm CO₂ compared with 350 ppm. Furthermore, although determined by different methods, their estimates of cell cycling times are comparable to ours, however, with a more pronounced CO₂ effect (20% change for a doubling in atmospheric [CO₂]).

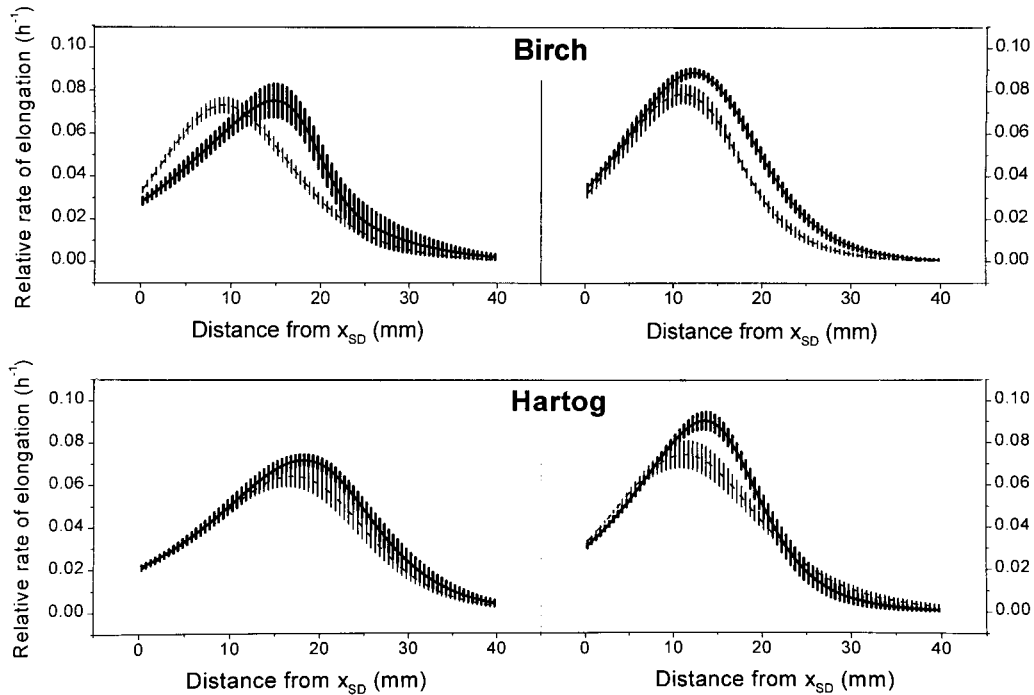


Figure 7. Relative elongation rates as a function of position along the “elongation-only” zone under 350 and 900 ppm CO₂ (thin and thick lines, respectively). Curves were fitted to averages calculated over groups of 20 cells; bars denote the corresponding SE values. Left, Vernalized seedlings; right, non-vernalized seedlings.

Elevated [CO₂] Affects Epidermal Cell Elongation Rate But Not Cell Length at Partitioning Nor Final Cell Length

Elevated [CO₂] also affected cellular growth in the meristem and beyond. This study reveals several new features about these effects. Growth [CO₂] influenced local rates of cell elongation but, remarkably, had no detectable effect on cell length at partitioning (l_{sd}), i.e. upon cell entry into the elongation-only zone (Fig. 6). Nor did it affect mature cell length (l_f , Table II) or width (data not shown). The elongation rates of meristematic cells were consistently increased by elevated [CO₂]. In non-vernalized leaves this stimulatory effect of elevated [CO₂] on wall elongation was maintained after cell migration out of the meristem (greater r_{max} , Fig. 7). In those leaves non-meristematic cells elongated faster under elevated [CO₂] but for a shorter time (Table III), with the net result being no change in l_f . In vernalized leaves, however, none of these effects of elevated [CO₂] was detectable. The maximum rate of cell elongation and the cell residence time in the elongation-only zone were insensitive to [CO₂] (Fig. 7; Table III), hence the conserved final cell length.

There are two possible hypotheses for the constancy of l_{sd} and l_f . The first hypothesis is that for cell partitioning to occur, meristematic cells have to reach a set threshold size and, once they have lost the ability to divide, cells elongate to a fixed length. Under that interpretation there is no direct sugar effect on cell cycling time or duration of cell elongation. Variations in t_c and T_{el} with growth [CO₂] follow from [CO₂] effects on cell elongation rates. In the absence of such effects, as in vernalized leaves (Fig. 7), T_{el} is unchanged. This first interpretation would require mech-

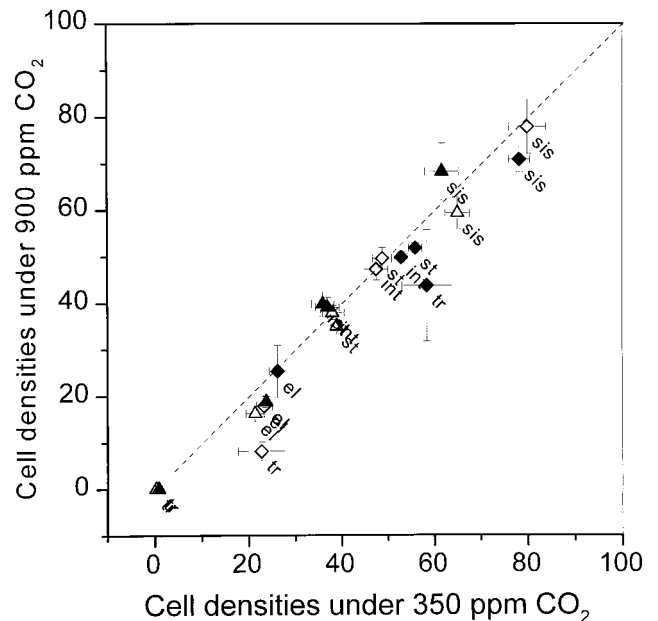


Figure 8. Densities of various epidermal cell types (no. of cells mm⁻²; means \pm SE) under 900 (y axis) and 350 ppm CO₂ (x axis) in cv Birch (triangles) and cv Hartog (diamonds). Black symbols denote data for vernalized leaves, white symbols those for non-vernalized leaves. Labels denote cell types: tr, trichomes; st, stomatal complexes; sis, sister cells (cell row adjacent to the stomatal rows); el, elongated non-specialized epidermal cells.

Table IV. Influence of growth $[CO_2]$ and vernalization on the length and projected area of mature mesophyll cells

Genotype	Vernalization	$[CO_2]$	Mesophyll Cell	
			Length	Projected area
			μm	μm^2
Birch	Yes	350	171a	3058b
		900	167a	3125bc
	No	350	163a	l
		900	160a	l
Hartog	Yes	350	122b	2746a
		900	109b	2812ab
	No	350	126b	3316c
		900	137b	3430c

anisms by which cells can measure their size. While there is some evidence for that in yeast (e.g. Nurse and Fantès, 1981), it is totally unknown whether such mechanisms operate in higher plants (Francis and Halford, 1995). Data from our other experiments (Beemster et al., 1996) have shown that there is no absolute size threshold for cell division in wheat, and no stable relationship between the partitioning rate and the elongation rate in meristematic cells.

The second hypothesis is that cell partitioning and cessation of growth are determined by the cell metabolic status and/or state of differentiation rather than by size per se. Under that interpretation, the concurrent decrease in \bar{t}_c (or T_{el}) and increase in r_{sd} (or r_{el}) observed under elevated $[CO_2]$ are caused by the increased metabolic activity associated with increased photoassimilate supply. The constancy of l_{sd} and l_f seen in this experiment would then simply mean that the rate of cell elongation and the rate at which a cell reaches the "critical" state, conditioning partitioning and cessation of growth, are increased by a similar proportion when cellular sugar concentrations increase. However, there is no reason to exclude the possibility that in other species and under different growth conditions, these two sets of parameters may show a differential sensitivity to sugars, leading to variations in l_{sd} or l_f as reported, for example, by Ferris et al. (1996) in perennial rye-grass under elevated $[CO_2]$ or by Beemster et al. (1996) in wheat under root stress. This second interpretation for the constancy of l_f in this experiment appeals to us in that it provides a unified explanation for the present data as well as others where l_{sd} and/or l_f have been found to vary. Furthermore, while not requiring any role of cell size per se it does not exclude it.

Whether direct or indirect a tight link between $[CO_2]$ effects on cell division and expansion processes is shown by the correlation between the spatial patterns of local rates of cell partitioning and cell elongation (Fig. 5). Furthermore, the fact that $[CO_2]$ effects on cell elongation are most important at the base of the meristem (Fig. 5) and smaller in the elongation zone indicates that these effects are modulated by factors related to cell position and/or meristematic status. Increased cellular Suc contents in the basal part of the growth zone may be one of these factors, as suggested by Schnyder and Nelson (1987) data in *Festuca*.

Elevated $[CO_2]$ Modifies Growth Anisotropy

Morphometric analysis of mature blade sections demonstrates that elevated $[CO_2]$ has more complex effects on cellular growth than revealed by the examination of cell lengths and does modify cell properties. Thus in cv Birch, while not affecting final cell lengths (Tables II and IV), elevated $[CO_2]$ caused a significant increase in the cross-sectional area of mesophyll cells and, in non-vernalized leaves, also of epidermal cells (Fig. 9). In cv Hartog, changes in mesophyll cell cross-sectional area were only observed in vernalized leaves. These observations lead to the suggestion that elevated $[CO_2]$ modifies the anisotropy of cell growth, and that the underlying control mechanisms are genetically variable and sensitive to factors influenced by exposure to low vernalizing temperatures. Moreover, the absence of a stable correlation between dimensional changes observed in epidermal and mesophyll cells (see Fig. 9) indicates that $[CO_2]$ effects on growth anisotropy may be in part tissue or even cell type specific.

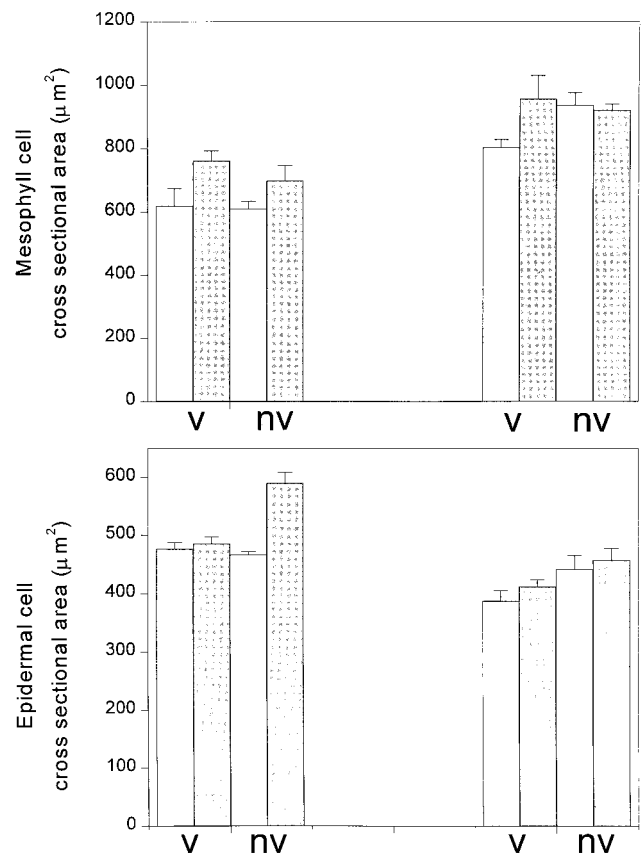


Figure 9. Mesophyll cell cross-sectional area (top panel; means and SE) and epidermal sister cells cross-sectional area (bottom panel) calculated as described in "Materials and Methods" in mature leaves grown under 350 (white bars) or 900 ppm CO_2 (gray bars). Data (means and SE) are shown for the two cultivars (left, cv Birch, and right, cv Hartog), and for vernalized and non-vernalized leaves (label v and nv on the x axis, respectively).

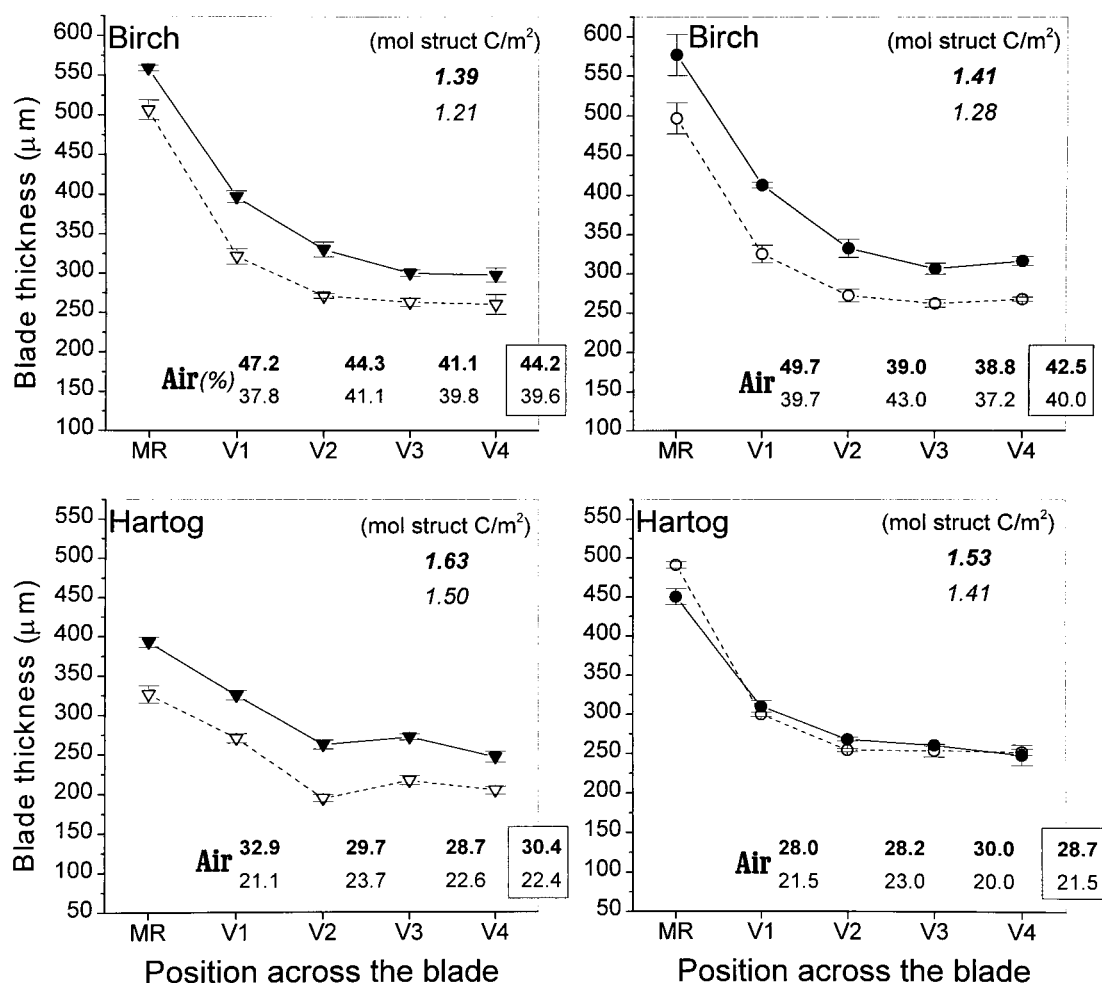


Figure 10. Decrease in blade thickness from the mid-rib to the edge of the blade. Measurements were taken on thin cross-sections across the mid-rib (MR) and the four adjacent veins (veins numbered 1–4 from MR) in mature leaves (leaf 6) grown under 350 or 900 ppm CO₂ (white and black symbols, respectively). Bars across symbols denote SE. The two rows of values above the x axis describe the extent of air spaces as a proportion of mesophyll tissue at the same locations (see “Materials and Methods”), with bold values (first row) referring to high-[CO₂]-grown leaves and the values below referring to leaves grown under 350 ppm CO₂. Boxed values are the averages across all positions. In the top right corner of each panel, average structural carbon contents (mol m⁻²) are given for high- and low-[CO₂]-grown blades (in bold and normal characters, respectively). Left, Vernalized seedlings; right, non-vernalized seedlings.

From Cells to Whole Leaf (Regulation of Whole-Leaf Elongation Rate)

The Enhancement of Leaf Growth Rate under Elevated [CO₂]: a Crucial Role of Effects in the Meristem

The kinematic methods of growth analysis provide a conceptual and mathematical framework for a quantitative analysis of the relationships between cell and whole-organ responses (Erickson and Sax, 1956; Green, 1976; Gandar, 1983a, 1983b) from two points of view:

First, whole leaf elongation, E , can be expressed as the integral of local strain rates, $r(x)$, over the length of the whole growth zone, with no explicit role of partitioning rate nor of the number of cells contributing to growth. This approach (Fig. 7) indicates that differences in E with growth [CO₂] arose in part from differences in the spatial regulation of cell wall elongation along the growth zone,

with elevated [CO₂] either up-regulating r at a given position without affecting the size of the growth zone (non-vernalized leaves), or displacing the peak of maximum cellular activity toward more distal positions along a longer growth zone (vernalized leaves).

Second, leaf elongation may also be seen as the integrals of growth activities of a certain number of cells, which sequentially move away from the meristem. Attention is now focused on the growth trajectories of individual material particles (cells here) with respect to time in considering that the endowment of a cell for elongation may be specified at the outset (e.g. see Van't Hof, 1973, and discussion in previous section) and that the size of the growth zone may be related to cell number rather than being physically fixed. This second approach, encapsulated in Equation 2, points to the importance in the present experiment of meristem size and activity in determining varia-

tions in leaf growth and anatomy with growth $[\text{CO}_2]$. With l_{sd} and l_f being highly conserved, variations in the overall elongations generated in the division and elongation-only zones were directly proportional to variations in cell flux, F . Furthermore, variations in final leaf length were proportional to those in total number of cells per file, i.e. in the number of proliferative divisions.

The importance of cell flux, often referred to as the cell production rate, in driving environmental effects on leaf expansion has been emphasized in several recent studies on roots (e.g. Muller et al., 1998), all of which concluded with the dominant role of changes in the number of cycling cells (N_{sd}) rather than changes in cell cycling rate (t_c). This cannot be generalized to the $[\text{CO}_2]$ -induced increase in epidermal cell fluxes observed in this study. The present data demonstrate that elevated $[\text{CO}_2]$ may affect both N_{sd} and t_c and that its relative impact on each parameter varies depending on genotype and vernalization treatment.

A Relative Insensitivity of Leaf Area Expansion to Elevated $[\text{CO}_2]$: CO_2 Effects on Leaf Anatomy

In all cases, at the leaf level, elevated $[\text{CO}_2]$ had relatively less effect on processes involved in expansive growth than on those determining growth in mass, leading to increased structural carbon content per unit leaf area (Fig. 10). This increase was not necessarily associated with increased blade thickness (e.g. in cv Hartog, non-vernalized leaves), a common characteristic of high- $[\text{CO}_2]$ -grown leaves (e.g. Downton et al., 1980; Thomas and Harvey, 1983). Increased carbon content was the overall result of, first, a large insensitivity of the final structure of the epidermis—a tissue thought to place major constraints on expansive growth in leaves (Kutschera et al., 1987)—to sugar supply. This insensitivity is manifest in the highly conserved epidermis anatomy, including stomatal density and cell dimensions in the paradermal leaf plane. Increased carbon content was also due to complex histological changes in the mesophyll tissue affecting both mesophyll cell initiation and development.

While the formation of an extra mesophyll cell layer under elevated $[\text{CO}_2]$ or an increase in mesophyll cell enlargement have been noted in other C_3 species (soybean, Thomas and Harvey, 1983; *Phaseolus*, Radoglou and Jarvis, 1992), the systematic increase in intercellular air spaces in high- $[\text{CO}_2]$ -grown leaves is an intriguing new finding. The formation of air spaces in leaves is generally thought to be developmentally regulated and to occur in a predictable manner involving localized lysis of cell wall components and local cell wall thickening (Knox, 1992; Raven, 1996). Its sensitivity to atmospheric $[\text{CO}_2]$ shown here is, however, consistent with experimental evidence and theoretical prediction that cell separation forces increase with cell turgor and cell diameter (Jarvis, 1998). Indeed, Suc contents were significantly greater in the high- $[\text{CO}_2]$ -grown leaves (Fig. 3), most likely resulting in increased mesophyll cell osmotic pressure and turgor; furthermore, in both cv Birch and cv Hartog, mesophyll cell diameter was increased.

While the formation of more numerous mesophyll cell layers under elevated $[\text{CO}_2]$ would allow increased carbon

deposition per unit leaf area, the greater extension of intercellular spaces plays in the opposite direction. The fact that leaf C/m^2 was increased even when this latter effect was the largest or even the only one to be significant, as in cv Hartog (non-vernalized leaves), implies that in these leaves, elevated $[\text{CO}_2]$ either increased carbon/unit cell wall area and/or increased the mesophyll cell area to volume ratio, through changes in cell lobing for example.

The significance of the anatomical changes induced in wheat leaves by elevated $[\text{CO}_2]$ for leaf function needs to be considered. Effects that contribute to increased leaf carbon/ m^2 constitute limitations to the magnitude of long-term whole-plant growth enhancement by elevated $[\text{CO}_2]$ (see equation 1 in Masle et al., 1990). On the other hand, more developed air spaces and increased cell area to volume ratio should facilitate CO_2 diffusion in the mesophyll tissue (Parkhurst, 1994), resulting in a smaller drop of CO_2 partial pressure between the substomatal cavity and sites of carboxylation, and thereby in higher effective assimilation rate at a given stomatal conductance.

$[\text{CO}_2]$ Effects on Leaf Growth Are Modified by Factors Related to Leaf Position, Vernalization, and Genotype

Genotypic Effects

There have been several recent reports of interspecific variation in growth responses to elevated $[\text{CO}_2]$ within a genus (*Populus*, Gardner et al., 1995; *Dactylis*, Kinsman et al., 1997). This study demonstrates intraspecific variation among cultivars of an intensively bred species. Genetic variation is shown in both the magnitude of $[\text{CO}_2]$ effects on a range of developmental processes and in the relative contributions of these processes to variations in leaf growth rate and anatomy. Our data, however, also reveal some highly conserved attributes, such as final cell length or number of epidermal cell files, which constrained leaf growth responses to elevated $[\text{CO}_2]$ in the two genotypes examined. These two groups of attributes define targets for an effective genetic manipulation of growth responses to $[\text{CO}_2]$ by classical breeding programs using natural genetic variation and by more directed genetic engineering.

Vernalization Effects

Aside from modifying the effects of atmospheric $[\text{CO}_2]$ on the size of the growth zone and on the kinetics of elongation within it, vernalizing temperatures had profound effects per se on overall blade elongation rate and mature blade anatomy. Unexpectedly, this was the case even in a genotype such as cv Hartog, classified as a spring type based on its vernalization requirements for flowering. In many respects, however, the effects of seed vernalization differed between cv Hartog and cv Birch, especially in the meristem. In the winter vernalized cv Birch leaves were characterized by a smaller meristem, comprising fewer epidermal cells with a faster partitioning rate than in non-vernalized seedlings (Table III) and smaller mesophyll cells (Table IV). In the spring cv Hartog, the opposite effects were observed, i.e. a longer meristem with more numerous

epidermal cells that cycled more slowly and thicker mesophyll cells. In the two genotypes, however, the two sets of effects resulted in only a small change in cell flux of similar direction (10% greater flux in non-vernalized seedlings). Vernalization systematically increased the residence time of cells in the elongation zone, especially under elevated [CO₂] (Table III), but caused a decrease in cell elongation rates (Fig. 7) so that final cell length remained mostly unchanged (Table II).

Overall, these data reveal that early exposure to low vernalizing temperatures affects the expression of a number of genes involved in leaf development and that these effects are modified by the plant carbohydrate status. Whether there is a direct link between the observed effects of low temperatures on leaf development and on vernalization per se, i.e. on the promotion of flowering, or whether these are independent effects is an open question. Several decades ago, Purvis and Hatcher (1959) observed in several cereals, including wheat, that vernalized seedlings had a shorter coleoptile and first leaf than non-vernalized ones. Since then, several genes controlling vernalization requirements in wheat have been identified (*vrn* genes), but studies of their expression have been restricted to a few genotypes with respect to flowering response and apical development only, with no attention being paid to possible pleiotropic effects on leaf development.

Leaf Position Effect

A feature common to all [CO₂] growth responses analyzed in this experiment is that significant [CO₂] effects on leaf elongation could not be detected in the first two to four leaves. A similar pattern was noted by Williams and Williams (1968) in their analysis of expansive growth under different light levels, and is also present in the data of Friend et al. (1962), which also showed variation in irradiance. How can this be explained? While it may be argued, following Williams (1960), that leaves 1 and 2 derive most of their carbon from seed reserves rather than from current photosynthesis, this is not the case for subsequent leaves. By the time leaf 3 emerges, seed reserves are depleted. Furthermore, as discussed earlier, the data presented in Figure 4 also rule out a direct causal relationship between the onset of tillering, which causes a sharp increase in carbon demand by axillary meristems and the appearance of a carbon limitation in the expanding leaves of the main tiller.

A third, non-exclusive interpretation is that the sensitivity of leaf growth to carbohydrates is developmentally regulated and is confined to early stages in leaf ontogeny. Recent molecular studies provide several examples of genes that are differentially regulated by sugars depending on the physiological/developmental context of the leaf (Kovtun and Daie, 1995). In the present experiments, leaves 1 to 5 all started to develop before sowing, i.e. before first exposure to different ambient [CO₂]. In wheat, leaves 1 to 3 are initiated in the embryo of the maturing seed, where their development is arrested by seed desiccation three to one plastochrons after initiation, respectively (Williams, 1960). Their development resumes slowly upon seed imbi-

tion and, in this experiment, during the subsequent period preceding sowing (see "Materials and Methods"). Over that period, which in thermal time was about 120 degree.days long (48 d at 2.5°C), two additional leaves were initiated (leaf 4, and just before sowing leaf 5, data not shown). On that basis we propose that the effects of sugars on the wheat leaf growth and final anatomy identified here may be largely determined in the leaf primordium, during the first three to five plastochrons of its development. Our recent observations on leaf development in relation to variations in root environment suggest a simple explanation for that. In a study on the effects of root impedance on leaf expansion in wheat (Masle, 1998), we found that a step change in soil strength only modified expansion growth and final leaf dimensions of those leaves which, upon imposition of the step change, were still enclosed in the whorl of older sheaths, i.e. were four to five plastochrons old at the most. We concluded that the kinetics of blade elongation and many attributes of the adult leaves were determined at these early stages. This explanation alone would lead one to expect, as observed in the present experiments, no to small CO₂ effects on all leaves initiated before exposure to high [CO₂], the more so in the older leaves. It would also account for the results of recently published studies where step changes in [CO₂] had no effect on the elongation rate of currently expanding leaves (e.g. Christ and Körner, 1995), leading to the erroneous conclusion that in wheat leaf growth per se is not carbon limited.

The data presented here demonstrate that elevated [CO₂] has profound effects on leaf development, expansive growth, and anatomy in wheat. They reveal that these effects are modulated by intrinsic factors related to genetic makeup and to leaf position, and by environmental cues important in apical development. They also identify important developmental constraints to the magnitude of whole-leaf responses to increased photoassimilate supply related to the controls of mature cell length, cell growth anisotropy, and number of cellular files contributing to lateral blade expansion. Similar types of interactions and limitations are likely to operate in many species (see the leaf position effect on expansion responses to elevated [CO₂] noted in bean by Leadley and Reynolds [1989]; see also the interactions between [CO₂] and photoperiodic requirements for flowering reported by Kinsman et al. [1997] in *Dactylis*). Their understanding holds the key to realistic predictions of vegetation (or even single species) responses to rising [CO₂] levels. It is also essential for the design of appropriate strategies for the engineering of genotypes most able to maximize the benefits of higher atmospheric [CO₂] in a given environment. More fundamentally, the elucidation of the functional bases of the novel interactions identified in this study is essential for understanding the role sugars play in the regulation of developmental genes under natural growth conditions.

ACKNOWLEDGMENTS

I thank Joanna Maleszka and Jason Chapman for superb technical assistance, Chin Wong and Peter Groeneveld for their work

in the design and computer control of the greenhouses, and Sandra Lavorel for her advice with statistical analysis of data.

Received August 19, 1999; accepted December 7, 1999.

LITERATURE CITED

- Ballard LAT, Wildman SG** (1964) Induction of mitosis by sucrose in excised and attached dormant buds of sunflower (*Helianthus annuus* L.). *Aust J Biol Sci* **17**: 36–43
- Beemster GTS, Masle J, Williamson RE, Farquhar GD** (1996) Effects of soil resistance to root penetration on leaf expansion in wheat (*Triticum aestivum* L.): kinematic analysis of leaf elongation. *J Exp Bot* **47**: 1663–1678
- Christ RA, Körner C** (1995) Responses of shoot and root gas exchange, leaf blade expansion and biomass production to pulses of elevated CO₂ in hydroponic wheat. *J Exp Bot* **46**: 1661–1667
- Downton WJ, Björkman O, Pike CS** (1980) Consequences of increased atmospheric concentrations of carbon dioxide for growth and photosynthesis of higher plants. In GI Pearman ed, *Carbon Dioxide and Climate: Australian Research*. Australian Academy of Science, Canberra, pp 143–151
- Erickson RO, Sax KB** (1956) Rates of cell division and cell elongation in the growth of the primary root of *Zea mays*. *Proc Am Philos Soc* **100**: 499–514
- Ferris R, Nijs I, Behaeghe T, Impens I** (1996) Elevated CO₂ and temperature have different effects on leaf anatomy of perennial ryegrass in spring and summer. *Ann Bot* **78**: 489–497
- Francis D, Halford NG** (1995) The plant cell cycle. *Physiol Plant* **93**: 365–374
- Friend DJC, Helson VA, Fisher JE** (1962) Leaf growth in Marquis wheat, as regulated by temperature, light intensity, and day-length. *Can J Bot* **40**: 1299–1311
- Gandar PW** (1983a) Growth in root apices: I. The kinematic description of growth. *Bot Gaz* **144**: 1–10
- Gandar PW** (1983b) Growth in root apices: II. Deformation and rate of deformation. *Bot Gaz* **144**: 11–19
- Gardner SDL, Taylor G, Bosac C** (1995) Leaf growth of hybrid poplar following exposure to elevated CO₂. *New Phytol* **131**: 81–90
- Goodwin RH, Stepka W** (1945) Growth and differentiation in the root tip of *Phleum pratense*. *Am J Bot* **32**: 36–46
- Green PB** (1976) Growth and cell pattern formation on an axis: critique of concepts, terminology, and modes of study. *Bot Gaz* **137**: 187–202
- Griffiths EW, Lyndon RF** (1985) The effects of vernalisation on the growth of the wheat shoot apex. *Ann Bot* **56**: 501–511
- Hewitt EJ, Smith TA** (1975) *Plant mineral nutrition*. English University Press, London
- Jarvis MC** (1998) Intercellular separation forces generated by intracellular pressure. *Plant Cell Environ* **21**: 1307–1310
- Jitla DS, Rogers GS, Seneweera SP, Basra AS, Oldfield RJ, Conroy JP** (1997) Accelerated early growth of rice at elevated CO₂: is it related to developmental changes in the shoot apex? *Plant Physiol* **115**: 15–22
- Kemp DR** (1980) The location and size of the extension zone of emerging wheat leaves. *New Phytol* **84**: 729–737
- Kinsman EA, Lewis C, Davies MS, Young JE, Francis D, Vilhar B, Ougham HJ** (1997) Elevated CO₂ stimulates cells to divide in grass meristems: a differential effect in two natural populations of *Dactylis glomerata*. *Plant Cell Environ* **20**: 1309–1316
- Knox JP** (1992) Cell adhesion, cell separation and plant morphogenesis. *Plant J* **2**: 137–141
- Kovtun Y, Daie J** (1995) End-product control of carbon metabolism in culture-grown sugar beet plants: molecular and physiological evidence of accelerated leaf development and enhanced gene expression. *Plant Physiol* **108**: 1647–1656
- Kutschera U, Bergfeld R, Schopfer P** (1987) Cooperation of epidermis and inner tissues in auxin-mediated growth of maize coleoptiles. *Planta* **170**: 168–180
- Leadley PW, Reynolds JF** (1989) Effect of carbon dioxide enrichment on development of the first six mainstem leaves in soybean. *Am J Bot* **76**: 1551–1555
- Masle J** (1984) Competition among tillers in winter wheat: consequences for growth and development of the crop. In W Day, RK Atkin, eds, *Wheat Growth and Modelling*. Plenum Press, NY, pp 33–54
- Masle J** (1998) Growth and stomatal responses of wheat seedlings to spatial and temporal variations in soil strength of bi-layered soils. *J Exp Bot* **49**: 1245–1257
- Masle J, Farquhar GD, Gifford RM** (1990) Growth and carbon economy of wheat seedlings as affected by soil resistance to penetration and ambient partial pressure of CO₂. *Aust J Plant Physiol* **17**: 465–487
- Masle J, Hudson GS, Badger MR** (1993) Effects of ambient CO₂ concentration on growth and nitrogen use in tobacco (*Nicotiana tabacum*) plants transformed with an antisense gene to the small subunit of ribulose-1,5-bisphosphate carboxylase/oxygenase. *Plant Physiol* **103**: 1075–1088
- Miller A, Tsai C-H, Hemphill D, Endres M, Rodermel S, Spalding M** (1997) Elevated CO₂ effects during leaf ontogeny. *Plant Physiol* **115**: 1195–1200
- Morris AK, Silk WK** (1992) Use of a flexible logistic function to describe axial growth of plants. *Bull Math Biol* **54**: 1069–1081
- Muller B, Stosser M, Tardieu F** (1998) Spatial distributions of tissue expansion and cell division rates are related to irradiance and to sugar content in the growing zone of maize roots. *Plant Cell Environ* **21**: 149–158
- Neales TF, Nicholls AO** (1978) Growth responses of young wheat plants to a range of ambient CO₂ levels. *Aust J Plant Physiol* **5**: 45–59
- Nicolas ME, Munns R, Samarakoon AB, Gifford RM** (1993) Elevated CO₂ improves the growth of wheat under salinity. *Aust J Plant Physiol* **20**: 349–360
- Nurse P, Fantes PA** (1981) Cell cycle controls in fission yeast: a genetic analysis. In PCL John, ed, *The Cell Cycle*. Society of Experimental Botany, Cambridge University Press, Cambridge, UK, pp 85–98
- Parker ML, Ford MA** (1982) The structure of the mesophyll of flag leaves in three *Triticum* species. *Ann Bot* **49**: 165–176
- Parkhurst DF** (1994) Diffusion of CO₂ and other gases inside leaves. *New Phytol* **126**: 449–479
- Purvis ON, Hatcher ESJ** (1959) Some morphological responses of cereal seedlings to vernalisation. *J Exp Bot* **10**: 277–289
- Radoglou KM, Jarvis PG** (1992) The effects of CO₂ enrichment and nutrient supply on growth morphology and anatomy of *Phaseolus vulgaris* L. seedlings. *Ann Bot* **70**: 245–256
- Raven JA** (1996) Into voids: the distribution, function, development and maintenance of gas spaces in plants. *Ann Bot* **78**: 137–142
- Robertson EJ, Leech RM** (1995) Significant changes in cell and chloroplast development in young wheat leaves (*Triticum aestivum* cv Hereward) grown in elevated CO₂. *Plant Physiol* **107**: 63–71
- Rogers HH, Cure JD, Thomas JF, Smith JM** (1984) Influence of elevated CO₂ on growth of soybean plants. *Crop Sci* **24**: 361–366
- Schnyder H, Nelson CJ** (1987) Growth rates and carbohydrate fluxes within the elongation zone of tall fescue leaf blades. *Plant Physiol* **85**: 548–553
- Schnyder H, Seo S, Rademacher IF, Kühbauch** (1990) Spatial distribution of growth rates and of epidermal cell lengths in the elongation zone during leaf development in *Lolium perenne* L. *Planta* **181**: 423–431
- Silk WK, Lord EM, Eckard KJ** (1989) Growth patterns inferred from anatomical records: empirical tests using longisections of roots of *Zea mays* L. *Plant Physiol* **90**: 708–713
- Sims DA, Seemann JR, Luo Y** (1998) Elevated CO₂ concentration has independent effects on expansion rates and thickness of soybean leaves across light and nitrogen gradients. *J Exp Bot* **49**: 583–591

- Skinner RH, Nelson CJ** (1995) Elongation of the grass leaf and its relationship to the phyllochron. *Crop Sci* **35**: 4–10
- Slafer GA, Rawson HM** (1997) CO₂ effects on phasic development, leaf number and rate of leaf appearance in wheat. *Ann Bot* **79**: 75–81
- Thomas JF, Harvey CN** (1983) Leaf anatomy of four species grown under continuous CO₂ enrichment. *Bot Gaz* **144**: 303–309
- Van't Hof J** (1973) The regulation of cell division in higher plants. *Brookhaven Symp* **25**: 152–165
- Vu JCV, Allen LH, Bowes G** (1989) Leaf ultrastructure, carbohydrates and protein of soybeans grown under CO₂ enrichment. *Environ Exp Bot* **29**: 141–147
- Webster PL, Henry M** (1987) Sucrose regulation of protein synthesis in pea root meristem cells. *Environ Exp Bot* **27**: 253–262
- Williams RF** (1960) The physiology of growth in the wheat plant: I. Seedling growth and the pattern of growth at the shoot apex. *Aust J Biol Sci* **13**: 401–428
- Williams RF, Williams CN** (1968) Physiology of growth in the wheat plant: IV. Effects of day length and light energy level. *Aust J Biol Sci* **21**: 835–854
- Wong SC, Kriedemann PE, Farquhar GD** (1992) CO₂ × nitrogen interaction on seedling growth of four species of eucalypt. *Aust J Bot* **40**: 457–472